Chapter 2
Time-Delayed Feedback Control

Chaos is found in greatest abundance wherever order is being sought. Chaos always defeats order because it is better organized.

Terry Pratchett

In the seminal work by Ott et al. [1], they demonstrated that small time-dependent changes of a parameter in a deterministic chaotic system can lead to periodic motion. Their findings are beyond classical control theory [2–5] and opened the field of chaos control which has become an aspect of increasing interest in nonlinear science [6, 7].

An especially powerful control scheme was introduced by Pyragas [8]. It is called time-delayed feedback control or time-delay autosynchronization and constructs a control force from the difference of the present state of a given system to its delayed value, i.e., $\mathbf{s}(t) - \mathbf{s}(t - \tau)$. For proper choices of the time delay τ, the control force vanishes if the state to be stabilized is reached. Thus, the method is noninvasive. This feedback scheme is easy to implement in an experimental setup and numerical calculation. It is capable of stabilizing fixed points as well as periodic orbits even if the dynamics are very fast. Furthermore, the Pyragas scheme has no need for a reference system since it generates the control force from information of the system itself. Also from a mathematical perspective it is an appealing instrument as the corresponding equations fall in the class of delay differential equations.

This chapter provides a summary of the time-delayed feedback scheme which is investigated in the subsequent chapters of this thesis and includes basic concepts for its analysis. Thus, it can be seen as the central node in this thesis and connects the other parts, where time-delayed feedback is applied to different classes of dynamic systems. The chapter is organized as follows: In Sect. 2.1, I will introduce the general concept of time-delayed feedback control starting with the original work by Pyragas [8]. Section 2.2 is devoted to extended time-delayed feedback invented by Socolar et al. [9]. This is an extension of the Pyragas scheme which will be used frequently in the subsequent chapters. Sections 2.3 and 2.4

P. Hövel, *Control of Complex Nonlinear Systems with Delay*,
Springer Theses, DOI: 10.1007/978-3-642-14110-2_2,

cover special realizations and further extensions of time-delayed feedback control. These include different coupling schemes, control loop latency, filtering, and nonlocal feedback. Section 2.5 describes the concept of linear stability analysis in the presence of time delay. This technique will be used several times in this thesis. Section 2.6 deals with the formalism of transfer functions and provides an additional perspective on the control mechanism. Finally, Sect. 2.7 concludes this chapter with an intermediate summary.

2.1 Control Method

In this section, I will discuss the time-delayed feedback method in its original form introduced by Pyragas [8]. The focus at this point is not the application of the control scheme to a specific system, but its introduction and general properties. The application to various classes of models will be the subject of the subsequent chapters.

Consider the following, general dynamic system

$$\frac{d}{dt}\mathbf{x}(t) = \mathbf{f}(\mathbf{x}(t)), \tag{2.1.1}$$

where $\mathbf{x}$ denotes a state vector of the n-dimensional state space, i.e., $\mathbf{x} \in \mathbb{R}^n$ and $\mathbf{f}$ is a function $\mathbf{f} : \mathbb{R}^n \to \mathbb{R}^n$ with $\mathbf{f} : \mathbf{x} \mapsto \mathbf{f}(\mathbf{x})$. In the following, I will present the above mentioned control method called time-delayed feedback control in a general notation. This method is also called time-delay autosynchronization or Pyragas control [8].

Figure 2.1 depicts a schematic diagram of the time-delayed feedback loop. The control parameters are given by the time delay τ, the feedback gain K, and in an extension of the Pyragas method the memory parameter R [9]. The red (dashed) color shows this extension of the original Pyragas control including multiple delays which will be discussed in Sect. 2.2. First, let me introduce the Pyragas control scheme.

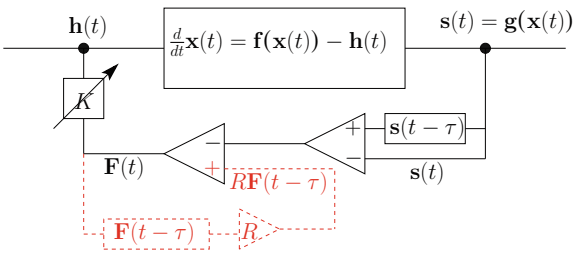

Fig. 2.1 Diagram of the time-delayed feedback control method. $\mathbf{x}(t)$ denotes the state of the system at time t, $\mathbf{s}(t)$ the control signal, i.e., some component of $\mathbf{x}(t)$ measured by $\mathbf{g}(\mathbf{x}(t))$, and $\mathbf{F}(t)$ is the control force. The real constants τ, K, and R denote the time delay, the feedback gain, and the memory parameter, respectively. The transducer function $\mathbf{h}(t)$ describes the coupling of $\mathbf{F}$ to the dynamic system $\mathbf{x}$. The extension of the original time-delayed feedback [8] as introduced by Socolar et al. (see Ref. [9]) is shown in *red* (*dashed*) color and discussed in Sect. 2.2

From the state vector $\mathbf{x} \in \mathbb{R}^n$, one can calculate a control signal $\mathbf{s} \in \mathbb{R}^m$ via a function $\mathbf{g} : \mathbb{R}^n \to \mathbb{R}^m$ with $\mathbf{g} : \mathbf{x} \mapsto \mathbf{s} = \mathbf{g}(\mathbf{x})$, which measures the state $\mathbf{x}$ to create a control signal in the m-dimensional signal space. This control signal could be, for instance, a single component of the state vector $\mathbf{x}$. The crucial part of the Pyragas control is to generate a control force $\mathbf{F}$ that consists of the difference between the current signal $\mathbf{s}(t)$ and a time-delayed counterpart $\mathbf{s}(t-\tau)$, i.e., $\mathbf{F} : \mathbb{R}^m \to \mathbb{R}^m$ with $\mathbf{F} : \mathbf{s} \mapsto \mathbf{s}(t) - \mathbf{s}(t-\tau)$. This control force is further multiplied by a control gain $K \in \mathbb{R}$. The application procedure of $\mathbf{F}$ to the dynamic system $\mathbf{x}$ is then specified by a transducer function $\mathbf{h} : \mathbb{R}^m \to \mathbb{R}^n$ with $\mathbf{h} : \mathbf{F} \mapsto \mathbf{h}(K\,\mathbf{F})$.

In a special realization of time-delayed feedback called diagonal control, for instance, the composition of the functions $\mathbf{g}$ and $\mathbf{h}$ becomes the identity, i.e., $\mathbf{h} \circ \mathbf{g} : \mathbb{R}^n \to \mathbb{R}^m \to \mathbb{R}^n$ with $\mathbf{h} \circ \mathbf{g} : \mathbf{x} \mapsto (\mathbf{h} \circ \mathbf{g})(\mathbf{x}) = \mathbf{h}(\mathbf{g}(\mathbf{x})) = \mathbf{x}$. Thus, for diagonal control the control force applied to the ith component of the system consists of the time-delayed difference of the same component. To summarize, the controlled system can be written as

$$\frac{d}{dt}\mathbf{x}(t) = \mathbf{f}(\mathbf{x}(t)) - \mathbf{h}[K\mathbf{F}(\mathbf{s}(t))] \tag{2.1.2a}$$

$$= \mathbf{f}(\mathbf{x}(t)) - \mathbf{h}[K(\mathbf{s}(t) - \mathbf{s}(t-\tau))] \tag{2.1.2b}$$

$$= \mathbf{f}(\mathbf{x}(t)) - \mathbf{h}[K\{\mathbf{g}(\mathbf{x}(t)) - \mathbf{g}(\mathbf{x}(t-\tau))\}]. \tag{2.1.2c}$$

Note that the difference term in the argument of $\mathbf{h}$ guarantees the noninvasive property of the control scheme which will be discussed next.

In order to investigate some properties of the control method, assume that the system $\mathbf{x}$ exhibits an unstable periodic orbit $\zeta(t)$ with period T which is meant to be stabilized via the Pyragas method. By choosing the time delay as $\tau = T$, the feedback method becomes noninvasive because the control force vanishes if the orbit ζ is stabilized: $\zeta(t) = \zeta(t-\tau) = \zeta(t-T)$. Let me stress the important feature once more: Only a minimum knowledge of the system $\mathbf{x}$ is required. The sole quantity of the system that needs to be known is the period T of the periodic orbit which determines the choice of the time delay. Methods to calculate the period of the target orbit a priori will be mentioned later in this section. Note that the exact knowledge of the unstable periodic orbit ζ is not necessary. This has the important consequence that invariant solutions of the uncontrolled system's equation persist unperturbed even in the presence of time-delayed feedback control. Only the neighborhood of the orbit is altered such that the dynamics converges to the target state.

The noninvasive property also holds if the desired state of the system is not a periodic orbit but a steady state $\mathbf{x}^*$ [10]. In the latter case, the control force also vanishes after reaching the stabilized state: $\mathbf{x}^*(t) \equiv \mathbf{x}^*(t-\tau)$. Optimal choice of the time delay are not so obvious as in the case of periodic orbits. This will be the topic of Chap. 3.

Instead of time-delayed feedback, it is tempting to use proportional feedback, where the control force $\mathbf{F}$ is given by the difference of the current state to the target state, for instance, a periodic orbit $\zeta(t)$

$$\mathbf{F}(t) = \mathbf{g}(\mathbf{x}(t)) - \mathbf{g}(\zeta(t)). \tag{2.1.3}$$

In order to apply this method, the orbit must be known a priori, e.g., reconstructed from experimental data or from a reference system, which eventually turns out to be a complicated process or is numerically expensive.

As mentioned above, the only quantity that needs to be known from the system is the period is the target orbit. There are various methods to calculate this period which then yields a promising choice of the time delay in the control loop. For instance, the feedback scheme itself can be used as a detection tool [11]. This might be interesting in an experimental setup, when a mathematical model in terms of differential equations is not at hand. In order to use the control method as a detection tool, the time delay needs to be varied. For the detection goal, the resonance behavior in terms of a vanishing control force $\mathbf{F}$ yields the desired period. Note that the occurrence of this resonance can be very sensitive with respect to small changes of the time delay [12–15].

One can also determine the period by optimization of a performance function which enables detection of unstable periodic orbits embedded in a strange attractor [16–18]. See also a comment on Ref. [16] and its reply [19, 20]. Alternatively, one can set up a few coupled equations relating the induced period, the true period, and the mismatched time delay by repeated application of an analytic approximation formula [21, 22] or by explicitly computing the unstable periodic orbit using a damped Newton solver [23].

Time-delayed feedback can also be used to explore a bifurcation diagram. Imagine a periodic which loses its stability as a bifurcation parameter is varied. This can happen, for instance, via a period-doubling cascade which subsequently leads to chaos. Without the control method, only the stable states would be visible in the bifurcation diagram. Applying time-delayed feedback could eventually stabilize a periodic orbit an area of the parameter space in which it would be unstable otherwise. This way, the periodic orbit can be tracked beyond the bifurcation point. Note, however, that the control parameters might need to be adjusted to follow the orbit in its previous unstable regime in the bifurcation parameter varies. This can be done by continuous change of the control parameters and this adjustment can even be performed automatically as was shown for periodic orbits in discrete as well as continuous systems [24, 25]. Let me stress that the target which is subject to the tracking procedure involving time-delayed feedback can also be a steady state as has been demonstrated numerically in Ref. [26] and experimental in an electrochemical system [27]. In addition, tracking by time-delayed feedback can also be used in spatio-temporal systems [28, 29].

To summarize, the main advantages of time-delayed feedback are the minimum knowledge of the investigated system and no need of a reference signal. In fact, the time-delayed feedback method generates the reference signal from the delayed time series of the system under control.

Another advantage of the control method is its easy experimental implementation. The control force can be realized, for instance, in a laser experiment

all-optically by an external resonator, where the propagation of the electric field in the cavity results in a time delay [30, 31], or opto-electronically by an additional electronic delay line [32, 33]. This enables stabilization of systems with fast dynamics. An additional electronic control loop with delay can be used for the control of electronic systems such as fast diode resonators [34, 35].

The easy experimental implementation shows that time-delayed feedback is superior to other control schemes. Consider, for instance, the famous OGY method named after its inventors Ott, Grebogi, and Yorke, which triggered the field of chaos control [1]. In their method, they showed how small perturbations of accessible parameters lead to a stabilization of periodic orbits in a chaotic system and thus turn previously chaotic motion into a stable periodic behavior. These perturbations are calculated such that the trajectory is pushed towards the desired orbit once it enters a neighborhood of this state. However, the difficulty is that one needs to calculate the unstable directions of the target state which in principle can be done by delay embedding, but they involve often time-consuming calculations. See Ref. [1]. These a priori calculations are not necessary for time-delayed feedback control.

Before discussing various extensions and modifications in the following sections, let me stress again that time-delayed feedback has been successfully employed in the context of chaos control. For a recent review including both basic aspects and applications see Ref. [7]. The applications cover various fields of research ranging from chaos communication, optics, electronic systems, chemical reactions, biology, and engineering.

2.2 Extended Time-Delayed Feedback

Socolar et al. [9] introduced an extension of the Pyragas method by taking states into account which are delayed by integer multiples of a basic time delay τ. This method is known as extended time-delayed feedback control or extended time-delay autosynchronization. Calculating the difference between two states which are one time unit τ apart yields the following control force [9, 36, 37]

$$\mathbf{F}(t) = \sum_{n=0}^{\infty} R^n [\mathbf{s}(t - n\tau) - \mathbf{s}(t - (n+1)\tau)] \tag{2.2.1a}$$

$$= \left[\mathbf{s}(t) - (1-R) \sum_{n=1}^{\infty} R^{n-1} \mathbf{s}(t - n\tau) \right] \tag{2.2.1b}$$

$$= [\mathbf{s}(t) - \mathbf{s}(t-\tau)] + R\mathbf{F}(t-\tau). \tag{2.2.1c}$$

The absolute value of the real constant R is smaller than unity, i.e., $|R| < 1$, such that it can be interpreted as a memory parameter that weights information of states further in the past. Note that the case $R = 0$ recovers the original Pyragas control scheme (2.1.2b). The equivalence of the three forms in (2.2.1a)–(2.2.1c) is shown

in the following. They can be done by reordering of the infinite series. First, I consider the derivation from (2.2.1a) to (2.2.1b):

$$\mathbf{F}(t) = \sum_{n=0}^{\infty} R^n[\mathbf{s}(t-n\tau) - \mathbf{s}(t-(n+1)\tau)] \tag{2.2.2a}$$

$$= \sum_{k=0}^{\infty} R^k \mathbf{s}(t-k\tau) - \sum_{m=0}^{\infty} R^m \mathbf{s}(t-(m+1)\tau) \tag{2.2.2b}$$

$$= \sum_{k=0}^{\infty} R^k \mathbf{s}(t-k\tau) - \sum_{m=1}^{\infty} R^{m-1} \mathbf{s}(t-m\tau) \tag{2.2.2c}$$

$$= \mathbf{s}(t) + \sum_{k=1}^{\infty} R^k \mathbf{s}(t-k\tau) - \sum_{m=1}^{\infty} R^{m-1} \mathbf{s}(t-m\tau) \tag{2.2.2d}$$

$$= \mathbf{s}(t) - \sum_{m=1}^{\infty} R^{m-1} \mathbf{s}(t-m\tau) - (-R) \sum_{k=1}^{\infty} R^{k-1} \mathbf{s}(t-k\tau) \tag{2.2.2e}$$

$$= \mathbf{s}(t) - (1-R) \sum_{n=1}^{\infty} R^{n-1} \mathbf{s}(t-n\tau). \tag{2.2.2f}$$

A similar derivation yields the third recursive form (2.2.1c) of the extended time-delayed feedback control force:

$$\mathbf{F}(t) = \sum_{n=0}^{\infty} R^n[\mathbf{s}(t-n\tau) - \mathbf{s}(t-(n+1)\tau)] \tag{2.2.3a}$$

$$= \underbrace{[\mathbf{s}(t) - \mathbf{s}(t-\tau)] - [\mathbf{s}(t) - \mathbf{s}(t-\tau)]}_{=0} \tag{2.2.3b}$$

$$+ \sum_{n=0}^{\infty} R^n[\mathbf{s}(t-n\tau) - \mathbf{s}(t-(n+1)\tau)] \tag{2.2.3c}$$

$$= \mathbf{s}(t) - \mathbf{s}(t-\tau) + \sum_{n=1}^{\infty} R^n[\mathbf{s}(t-n\tau) - \mathbf{s}(t-(n+1)\tau)] \tag{2.2.3d}$$

$$\begin{aligned} &= \mathbf{s}(t) - \mathbf{s}(t-\tau) + \sum_{n=0}^{\infty} R^{n+1}[\mathbf{s}(t-(n+1)\tau) - \mathbf{s}(t-(n+2)\tau)] \\ &= [\mathbf{s}(t) - \mathbf{s}(t-\tau)] + R \underbrace{\sum_{n=0}^{\infty} R^n[\mathbf{s}(t-n\tau-\tau) - \mathbf{s}(t-(n+1)\tau-\tau)]}_{=\mathbf{F}(t-\tau)} \\ &= [\mathbf{s}(t) - \mathbf{s}(t-\tau)] + R\mathbf{F}(t-\tau). \end{aligned} \tag{2.2.3e}$$

Although the first form of the extended time-delayed feedback force (2.2.1a) can be seen as an analogy of the Pyragas control, this form is not feasible for numerical implementation because it requires to store information of all states in the past. However, there is also the equivalent recursive form given in (2.2.1c) which involves next to the time-delayed control signal $\mathbf{s}(t-\tau)$ the delayed version of the control force $\mathbf{F}(t-\tau)$ itself. This form becomes more suitable for an experiment. The extension of the original time-delayed feedback scheme is depicted schematically in Fig. 2.1, where the red dashed color displays the additional recursion component according to (2.2.1c). In an all-optical experimental setup, the feedback scheme in its extended form can be realized by a Fabry–Perot resonator as will be discussed in Sect. 3.5.3.

It is worth noting that, similar to time-delayed feedback, the extended version possesses the noninvasive property. The control force vanishes if the target state, e.g., periodic orbit or steady state, is stabilized. Thus, the target states are invariant solutions of the uncontrolled system which persist unperturbed in the presence of (extended) time-delayed feedback. The delayed feedback can also induce additional solutions which are not solutions of the uncontrolled system. For these delay-induced states, the control scheme is invasive and the control force does not vanish. They are important if the corresponding modes become dominant and are used in Chap. 4 in an exchange of stability with the orbit to be stabilized.

So far, nothing was said about the specific choice of the coupling function $\mathbf{g}$ which extracts information of the system to generate a control signal and the transducer function $\mathbf{h}$ which determines the realization of the feedback scheme. This topic will be discussed in the next section.

2.3 Coupling Schemes

In the framework of, for instance, neural systems of 2-variable activator–inhibitor type as it will be investigated in Chap. 6, it is of crucial importance to carefully distinguish between different coupling schemes. First of all, there is a difference by generating the control signal form the inhibitor or the activator variable. In addition, the application of the control force to the system leaves again the choice of coupling to the activator or the inhibitor. Depending on the specific realization of the coupling, one can expect different responses of the system to the control scheme [38, 39].

In order to discuss the roles of the coupling function $\mathbf{g}$ and the transducer function $\mathbf{h}$, it is convenient to rewrite (2.1.2b) of the controlled system in vector form:

$$\frac{d}{dt}\mathbf{x}(t) = \mathbf{f}(\mathbf{x}(t)) - \mathbf{h}[K(\mathbf{s}(t) - \mathbf{s}(t-\tau))] \tag{2.3.1a}$$

$$\begin{pmatrix} \dot{x}_1(t) \\ \vdots \\ \dot{x}_n(t) \end{pmatrix} = \begin{pmatrix} f_1(x_1(t),\ldots,x_n(t)) \\ \vdots \\ f_n(x_1(t),\ldots,x_n(t)) \end{pmatrix} - \begin{pmatrix} h_1[K(s_1(t)-s_1(t-\tau)),\ldots,K(s_m(t)-s_m(t-\tau))] \\ \vdots \\ h_n[K(s_1(t)-s_1(t-\tau)),\ldots,K(s_m(t)-s_m(t-\tau))] \end{pmatrix}, \tag{2.3.1b}$$

where $x_i(t)$ denotes the ith component of the state vector $\mathbf{x}(t) = (x_i(t),\ldots,x_i(t))^T$ and similar notations hold for **f**, **g**, **h**, and **s**, where the function **g** is given by

$$\mathbf{g}(\mathbf{x}(t)) = \begin{pmatrix} g_1(x_1(t),\ldots,x_n(t)) \\ \vdots \\ g_m(x_1(t),\ldots,x_n(t)) \end{pmatrix} \tag{2.3.2}$$

with $g_i : \mathbb{R}^m \to \mathbb{R}$, $g_i : x_1,\ldots,x_n \mapsto s_i = g_i(x_1,\ldots,x_n)$ for each vector element $i = 1$, ..., m. A similar notation can be applied to Eqs. 2.1.2a and 2.1.2c as well. For a schematic diagram of the control method see Fig. 2.1. This notation seems lengthy, but it can be shortened assuming that **g** and **h** are linear functions which can be written as matrices with proper dimensions, i.e., **g** becomes a $n \times m$ matrix and **h** turns into a $m \times n$ matrix. Then, (2.3.1b) can be rewritten as

$$\begin{pmatrix} \dot{x}_1(t) \\ \vdots \\ \dot{x}_n(t) \end{pmatrix} = \begin{pmatrix} f_1(x_1(t),\ldots,x_n(t)) \\ \vdots \\ f_n(x_1(t),\ldots,x_n(t)) \end{pmatrix} - K \begin{pmatrix} h_{11} & \cdots & h_{1m} \\ \vdots & \ddots & \vdots \\ h_{n1} & \cdots & h_{nm} \end{pmatrix} \times \begin{pmatrix} g_{11} & \cdots & g_{1n} \\ \vdots & \ddots & \vdots \\ g_{m1} & \cdots & g_{mn} \end{pmatrix} \begin{pmatrix} x_1(t)-x_1(t-\tau) \\ \vdots \\ x_n(t)-x_n(t-\tau) \end{pmatrix} \tag{2.3.3a}$$

such that the equation for the ith component of the state vector **x** becomes

$$\frac{dx_i(t)}{dt} = f_i(x_1(t),\ldots,x_n(t)) - K\sum_{j=1}^{n} \mathbf{A}_{ij}[x_j(t)-x_j(t-\tau)] \tag{2.3.4a}$$

$$\frac{d}{dt}\mathbf{x}(t) = \mathbf{f}(\mathbf{x}(t)) - K\mathbf{A}[\mathbf{x}(t)-\mathbf{x}(t-\tau)], \tag{2.3.4b}$$

where the elements of the $n \times n$ coupling matrix **A** are given by

$$\mathbf{A}_{ij} = \sum_{k=1}^{m} h^{ik} g_{kj}. \tag{2.3.5}$$

This matrix selects which components of $\mathbf{x}$ are used for construction of the control signal and specifies the application of the control force back to the system.

The function $\mathbf{g} = (g_1, \ldots, g_m)^T$ determines which components of the system $\mathbf{x}$ are measured to generate the difference to the time-delayed signal. In the simplest case, g_i extracts the ith component of $\mathbf{x}$:

$$g_i(x_1(t), \ldots, x_j(t), \ldots, x_n(t)) = x_i(t)\delta_{i,j} \qquad \forall i,j = 1, \ldots, n. \tag{2.3.6}$$

If $h_i = KF_i$ also selects the ith component, then this coupling scheme is called diagonal.

The control signal $\mathbf{s} = (s_1, \ldots, s_m)^T$ can also contain global information of the system. In this case of global control, $\mathbf{g}$ yields, for instance, the calculation of the average of the system components or mean field:

$$g_i(x_1(t), \ldots, x_n(t)) = \frac{1}{n}\sum_{k=1}^{n} x_k(t) \qquad \forall i = 1, \ldots, n. \tag{2.3.7}$$

This kind of control signal is often used in the context of networks, where a measurement of a single node is not possible. Global delayed feedback is applied, for instance, to coupled phase oscillators of Kuramoto type [40, 41], Hindmarsh-Rose neurons [42], and limit cycle oscillators [43, 44]. It is also of importance for the class of spatio-temporal systems, when a spatial variable is not accessible, but an overall current turns out to be a convenient choice for the control signal [15, 28, 45–56]. In these spatio-temporal systems, the coupling function $\mathbf{g}$ involves a spatial average which can be realized by an integral, for instance, in one-dimensional systems:

$$\mathbf{g}(\mathbf{x}(x,t)) = \int_0^L \mathbf{x}(x,t)\, dx, \tag{2.3.8}$$

where L denotes a constant length which determines the spatial dimension of the system. Different local and global coupling schemes were systematically compared in Refs. [28, 45].

The function $\mathbf{g}$ can also act as a differential operator if the derivative of $\mathbf{x}$ is accessible in an experiment. In Chap. 5, for instance, the second derivative enters the control signal and thus, $\mathbf{g}$ reads:

$$g_i(x_1(t), \ldots, x_j(t), \ldots, x_n(t)) = \ddot{x}_i(t)\delta_{i,j} \qquad \forall i,j = 1, \ldots, n. \tag{2.3.9}$$

Other choices of $\mathbf{g}$ will be discussed later in this section and in the subsequent chapters for various classes of dynamic systems.

While the function $\mathbf{g}$ specifies the generation of the control signal $\mathbf{s}$, the transducer function $\mathbf{h} = (h_1, \ldots, h_n)^T$ with $h_i : \mathbb{R}^m \to \mathbb{R}$, $h_i : s_1, \ldots, s_m \mapsto h_i(s_1, \ldots, s_m)$ ($i = 1, \ldots, m$) determines the component of the system to which the control force is applied. In optical system, some components of the system's state $\mathbf{x}$ describes the

electric field. In this context, **h** takes into account changes of the polarization axis. This will be discussed in detail in Sect. 3.5, where an additional phase parameter comes into play [30, 57, 58].

In the field of networks, when $x_i(t)$ describes the dynamics of the ith node and can be understood as a vector quantity itself, prominent choices of the function **h** include all-to-all coupling and nearest-neighbor coupling. In the first case, all components of **h** are identical. In the latter case, **h** connects only nodes which are next to each other in the network. In a one-dimensional ring configuration, for instance, the function **h** can be written as

$$h_i[K\mathbf{F}(\mathbf{s}(t))] = K(s_j(t) - s_j(t-\tau))\big(\delta_{i-1,j} + \delta_{i+1,j}\big), \tag{2.3.10}$$

where s_{n+1} and s_0 are identified with s_1 and s_n by periodic boundary condition, respectively. In terms of a coupling matrix **A** as in Eqs. 2.3.4, Equation 2.3.10 corresponds to a matrix with only secondary diagonal entries, i.e., $a_{i,i\pm1} = 1$ for all $i = 1, ..., n$. The two choices of all-to-all coupling and nearest-neighbor coupling serve also as paradigmatic case for global and local control.

In the linear case of **g** and **h**, the two functions could be merged into a single control function. If **h** becomes nonlinear, however, this is not possible anymore because of the noninvasive property and hence, the main advantage of time-delayed feedback would be lost.

Before turning towards extensions of time-delayed feedback, let me discuss further examples of **g** and **h**. Next to the already mentioned case, where g_i extracts the ith component of the system, **g** can also be used to construct the control signal from a single component only, i.e., **g** is given for fixed $i \in 1, ..., n$ by

$$g_i(x_1(t), \ldots, x_j(t), \ldots, x_n(t)) = x_j(t) \quad \text{and} \quad g_k \equiv 0 \quad \text{for} \quad k \neq i. \tag{2.3.11}$$

As an example of this choice, see Ref. [59], where the chaotic Rössler system (with real constants a, b, and μ) is subject to time-delayed feedback in the following realization

$$\begin{aligned}\begin{pmatrix}\dot{x}_1(t)\\ \dot{x}_2(t)\\ \dot{x}_3(t)\end{pmatrix} &= \begin{pmatrix}-x_2(t) - x_3(t)\\ x_1(t) + a x_2(t)\\ b + x_3(t)(x_1(t) - \mu)\end{pmatrix}\\ &\quad - K\underbrace{\begin{pmatrix}1 & 0 & 0\\ 0 & 0 & 0\\ 0 & 0 & 0\end{pmatrix}}_{=\mathbf{A}}\begin{pmatrix}x_1(t) - x_1(t-\tau)\\ x_2(t) - x_2(t-\tau)\\ x_3(t) - x_3(t-\tau)\end{pmatrix}.\end{aligned} \tag{2.3.12}$$

One can see the composition $\mathbf{h} \circ \mathbf{g}$ yields a 3×3 matrix **A** with only one non-zero element.

Another special realization that will become important and act as a reference case in the following chapters is called diagonal control. In this choice, the control force applied to the ith component of the system consists only of

information of the same component and thus, the composition of the functions $\mathbf{g}$ and $\mathbf{h}$, i.e., the coupling matrix $\mathbf{A}$, is the identity. Then, the controlled system can be simplified to

$$\frac{d}{dt}\mathbf{x}(t) = \mathbf{f}(\mathbf{x}(t)) - K\mathbf{A}[\mathbf{x}(t) - \mathbf{x}(t-\tau)] \tag{2.3.13a}$$

$$\begin{aligned} \Leftrightarrow \begin{pmatrix} \dot{x}_1(t) \\ \vdots \\ \dot{x}_n(t) \end{pmatrix} &= \begin{pmatrix} f_1(x_1(t), \ldots, x_n(t)) \\ \vdots \\ f_n(x_1(t), \ldots, x_n(t)) \end{pmatrix} \\ &\quad - K \begin{pmatrix} 1 & & \mathbf{0} \\ & \ddots & \\ \mathbf{0} & & 1 \end{pmatrix} \begin{pmatrix} x_1(t) - x_1(t-\tau) \\ \vdots \\ x_n(t) - x_n(t-\tau) \end{pmatrix} \\ &= \begin{pmatrix} f_1(x_1(t), \ldots, x_n(t)) \\ \vdots \\ f_n(x_1(t), \ldots, x_n(t)) \end{pmatrix} - K \begin{pmatrix} x_1(t) - x_1(t-\tau) \\ \vdots \\ x_n(t) - x_n(t-\tau) \end{pmatrix}. \end{aligned} \tag{2.3.13b}$$

The example of the Rössler system given above can be seen as a simplification of diagonal control because only a single diagonal entry of the coupling matrix is non-zero.

In optical systems as mentioned above, the polarization leads to a phase-dependent coupling. This can be realized by the introduction of a control phase φ and the controlled system is then given by

$$\begin{aligned} \begin{pmatrix} \dot{x}_1(t) \\ \dot{x}_2(t) \\ \vdots \\ \dot{x}_n(t) \end{pmatrix} &= \begin{pmatrix} f_1(x_1(t), \ldots, x_n(t)) \\ f_2(x_1(t), \ldots, x_n(t)) \\ \vdots \\ f_n(x_1(t), \ldots, x_n(t)) \end{pmatrix} \\ &\quad - K \begin{pmatrix} \cos\varphi & \sin\varphi & \mathbf{0} & \ldots & \mathbf{0} \\ -\sin\varphi & \cos\varphi & \mathbf{0} & \ddots & \vdots \\ \mathbf{0} & \mathbf{0} & \mathbf{0} & \ddots & \vdots \\ \vdots & \ddots & \ddots & \ddots & \vdots \\ \mathbf{0} & \ldots & \ldots & \ldots & \mathbf{0} \end{pmatrix} \begin{pmatrix} x_1(t) - x_1(t-\tau) \\ x_2(t) - x_2(t-\tau) \\ \vdots \\ x_n(t) - x_n(t-\tau) \end{pmatrix}, \end{aligned} \tag{2.3.14}$$

where x_1 and x_2 correspond to the real and imaginary parts of the electric field, respectively [30, 57, 58]. This will be investigated in detail in Sect. 3.5. Note that the choice $\varphi = 0$ recovers the diagonal control.

After the discussion of different realizations of the time-delayed feedback scheme, I will add some remarks on further extensions of this control method in the next section.

2.4 Extensions

In this section, I will summarize some aspects concerning possible modifications of the original time-delayed feedback control scheme as introduced in Sect. 2.1 and given by (2.1.2). These extensions include, without claim of completeness latency time effects, filtering of the control signal, multiple time delays, and nonlocal coupling.

Previously, I have assumed that the generation of the feedback and its application to the system under control happens instantaneously. In an experimental setup, however, there is always a latency involved. This control loop latency is associated with finite propagation speed of the control signal, delays in the measurement of the system to generate the control signal, or processing times for the calculation of the feedback [10, 57, 58, 60, 61]. In optical or opto-electronic systems, for instance, the length of an optical fiber used to transmit the control signal can become of crucial importance [35]. The same holds for electronic systems such as a fast diode resonator, where also a propagation delay act as limiting factor [34]. In neuronal systems, these propagation delays, e.g., in dendrites, play also an important role both in models and experiments [62, 63].

All latency times of different origins can be summed up to a new control parameter δ which acts as an additional time delay in all arguments of the control loop. Therefore, the controlled system of (2.1.2) can be rewritten as

$$\frac{d}{dt}\mathbf{x}(t) = \mathbf{f}(\mathbf{x}(t)) - \mathbf{h}[K\mathbf{F}(\mathbf{s}(t-\delta))] \tag{2.4.1a}$$

$$= \mathbf{f}(\mathbf{x}(t)) - \mathbf{h}[K(\mathbf{s}(t-\delta) - \mathbf{s}(t-\delta-\tau))] \tag{2.4.1b}$$

$$= \mathbf{f}(\mathbf{x}(t)) - \mathbf{h}[K\{\mathbf{g}(\mathbf{x}(t-\delta)) - \mathbf{g}(\mathbf{x}(t-\delta-\tau))\}]. \tag{2.4.1c}$$

Note that the problem of latency cannot be solved by the introduction of a rescaled time delays $\tilde{\tau}$, i.e., $\tilde{\tau} = \delta + \tau$, because the quantity δ occurs also in the argument of both $\mathbf{s}(t-\delta)$ and $\mathbf{s}(t-\delta-\tau)$. This issue will be elaborated in Sect. 3.4 in the context of stabilization of steady states. I will derive an analytical expression of upper bound for δ, i.e., a maximum latency time, such that control is still possible [10, 57, 58].

Another issue that needs to be taken into account is additional filter in the control loop. On the one hand, the reason can be a limited bandwidth of the experimental equipment such that filtering is unavoidable. On the other hand, filters can be built into the control loop on purpose. In the latter case, the aim is to

reduce the influence of unwanted high frequencies in the control force which eventually lead to the stabilization of the wrong timescales. If, for instance, these high frequencies are present in the system and yield generation of a feedback with the same fast timescale, a low-pass filter can help to overcome this limitation [13, 14, 49]. To adjust the time-delayed feedback scheme to this obstacle, the control signal $\mathbf{s}$ in (2.1.2) needs to be replaced by a low-pass filtered version $\overline{\mathbf{s}}$ and the controlled system reads:

$$\frac{d}{dt}\mathbf{x}(t) = \mathbf{f}(\mathbf{x}(t)) - \mathbf{h}[K\mathbf{F}(\overline{\mathbf{s}}(t))] \tag{2.4.2a}$$

$$= \mathbf{f}(\mathbf{x}(t)) - \mathbf{h}[K(\overline{\mathbf{s}}(t) - \overline{\mathbf{s}}(t-\tau))], \tag{2.4.2b}$$

where the low-pass filter can be described in different ways. On one hand, it can be realized by an additional differential equation as follows:

$$\frac{d}{dt}\overline{\mathbf{s}}(t) = -\alpha\overline{\mathbf{s}}(t) + \alpha\mathbf{s}(t), \tag{2.4.3}$$

where α denotes the cutoff frequency of the filter. On the other hand, there exists an equivalent integral formula for $\overline{\mathbf{s}}$:

$$\overline{\mathbf{s}}(t) = \alpha \int_{-\infty}^{t} \mathbf{s}(t')e^{-\alpha(t-t')}\,dt'. \tag{2.4.4}$$

The equivalence can be seen by straight forward calculation inserting (2.4.4) into (2.4.3)

$$\frac{d}{dt}\overline{\mathbf{s}}(t) = \frac{d}{dt}\alpha \int_{-\infty}^{t} \mathbf{s}(t')e^{-\alpha(t-t')}\,dt' \tag{2.4.5a}$$

$$= \left[\frac{d}{dt}e^{-\alpha t}\right]\alpha \int_{-\infty}^{t} \mathbf{s}(t')e^{\alpha t'}\,dt' + e^{-\alpha t}\alpha\frac{d}{dt}\left[\int_{-\infty}^{t} \mathbf{s}(t')e^{\alpha t'}\,dt'\right]$$

$$= \underbrace{-\alpha\, e^{-\alpha t}\alpha \int_{-\infty}^{t} \mathbf{s}(t')e^{\alpha t'}\,dt'}_{\overline{\mathbf{s}}(t)} + \underbrace{e^{-\alpha t}\alpha\mathbf{s}(t)e^{\alpha t}}_{\alpha\mathbf{s}(t)} \tag{2.4.5b}$$

$$= -\alpha\overline{\mathbf{s}}(t) + \alpha\mathbf{s}(t). \tag{2.4.5c}$$

Alternatively, the solution of the linear, inhomogeneous, differential equation (2.4.3) can be written as

$$\bar{\mathbf{s}}(t) = \int_{-\infty}^{\infty} G(t-t')\mathbf{s}(t')\,dt' \tag{2.4.6}$$

with the Green's function

$$G(t) = \begin{cases} \alpha e^{-\alpha t}, & t \geq 0 \\ 0, & t < 0 \end{cases}, \tag{2.4.7}$$

which yields the integral formula (2.4.4). This issue will be become important again in Sect. 2.6, where a transfer function of the low-pass filter will be derived.

Similar to a low-pass filter, one can think of the introduction of a high-pass filter or a bandpass filter into the control loop [64, 65]. In optical systems, filtering of the feedback signal was also investigated for laser models of Lang–Kobayashi type [66, 67]. Furthermore, the introduction of a filtered feedback has also been proven to be important in the investigation of a Hopf bifurcation [33].

If there are multiple timescales in the system that need to be controlled, the introduction of additional control loops with different time delays τ_1, τ_2, ... can be a proper extension. In this case, there will be a complex interplay between the different timescales [68–71].

A second time delay needs also to be taken into account, if it is already part of the dynamics of the uncontrolled system:

$$\frac{d}{dt}\mathbf{x}(t) = \mathbf{f}(\mathbf{x}(t), \mathbf{x}(t-\tau_1)). \tag{2.4.8}$$

In this case, the delay τ_2 of the time-delayed feedback scheme can be chosen independently:

$$\frac{d}{dt}\mathbf{x}(t) = \mathbf{f}(\mathbf{x}(t), \mathbf{x}(t-\tau_1)) - \mathbf{h}[K(\mathbf{s}(t) - \mathbf{s}(t-\tau_2))], \tag{2.4.9a}$$

An example, where the intrinsic time delay occurs in the highest derivative, will be considered in Chap. 5. See also Refs [72, 73].

It is also of importance to consider the limits of small and large time delays. In the limit of vanishing τ and assuming the feedback gain is of the order τ^{-1}, i.e., $K = O(1/\tau)$, the time-delayed feedback force becomes

$$\lim_{\tau\to 0} K\mathbf{F}(\mathbf{s}(t)) = \lim_{\tau\to 0} K[\mathbf{s}(t) - \mathbf{s}(t-\tau)] \tag{2.4.10a}$$

$$= \tilde{K} \lim_{\tau\to 0} \frac{\mathbf{s}(t) - \mathbf{s}(t-\tau)}{\tau} \tag{2.4.10b}$$

$$= \tilde{K} \frac{d\mathbf{s}(t)}{dt} \tag{2.4.10c}$$

$$= \tilde{K} \frac{d\mathbf{g}(\mathbf{x}(t))}{dt}. \tag{2.4.10d}$$

Thus, the control force is proportional to the derivative of the control signal and the time-delayed feedback methods is equal to derivative control [74–76]. Derivative control has a disadvantage that it is sensitive to high frequencies. This becomes clear from the Fourier transform of (2.4.10c):

$$\mathcal{F}\left[\frac{d\mathbf{s}(t)}{dt}\right] = \int_{-\infty}^{\infty} \frac{d\mathbf{s}(t)}{dt} e^{-i\omega t}\, dt \tag{2.4.11a}$$

$$= \mathbf{s}(t)e^{-i\omega t}\Big|_{-\infty}^{\infty} - \int_{-\infty}^{\infty} \mathbf{s}(t)\frac{d}{dt}e^{-i\omega t}\, dt \tag{2.4.11b}$$

$$= i\omega \int_{-\infty}^{\infty} \mathbf{s}(t)e^{-i\omega t}\, dt \tag{2.4.11c}$$

$$= i\omega\mathcal{F}[\mathbf{s}(t)] \tag{2.4.11d}$$

$$= i\omega\hat{\mathbf{s}}(\omega), \tag{2.4.11e}$$

where $\hat{\mathbf{s}}$ denotes the Fourier transform of the control signal $\mathbf{s}$. For instance in the presence of noise including high frequencies ω, this could lead to an arbitrarily large control force.

The second limit of large time delays, i.e., $\tau \to \infty$, will be discussed in Sect. 3.6 in the context of stabilization of steady states, when I will investigate the asymptotic behavior of the eigenvalues in the presence of time-delayed feedback.

I want to mention at last an extension to systems that have also spatial degrees of freedom. In these spatio-temporal systems, the feedback scheme can still be used in the previously discussed time-delayed form. However, it is also possible to use the spatial coordinate and a space delay Δx to generate a nonlocal control force. Restricting the discussion for notational convenience to systems $\mathbf{x}(x, t)$ with one spatial dimension, the control force $\mathbf{F}(x, t)$ can be written in analogy to the time-delayed case of (2.1.2c)

$$\mathbf{F}(x,t) = \mathbf{s}(x,t) - \mathbf{s}(x - \Delta x, t) \tag{2.4.12a}$$

$$= \mathbf{g}(\mathbf{x}(x,t)) - \mathbf{g}(\mathbf{x}(x - \Delta x, t)), \tag{2.4.12b}$$

where Δx denotes the spatial delay, i.e., the distance of the nonlocal coupling. This method was used for stabilization of unstable periodic pattern in spatio-temporal chaos in optical systems [77] as well as in neuronal systems [38, 78–80].

Opposed to the purely time-dependent case, where only information of the past is accessible, one can introduce in spatio-temporal systems a feedback which is symmetric in space

$$\mathbf{F}(x,t) = -\mathbf{s}(x + \Delta x, t) + 2\mathbf{s}(x,t) - \mathbf{s}(x - \Delta x, t) \tag{2.4.13a}$$

$$= -\mathbf{g}(\mathbf{x}(x - \Delta x, t)) + 2\mathbf{g}(\mathbf{x}(x,t)) - \mathbf{g}(\mathbf{x}(x - \Delta x, t)). \tag{2.4.13b}$$

Further variations of the space-delayed feedback are possible. In general form, all different realization can be summarized using an integral kernel $\kappa(x')$ which specifies the coupling. Then, the control force can be written in a one-dimensional system as

$$\mathbf{F}(x,t) = \int_0^\infty \kappa(x')[\mathbf{s}(x,t) - \mathbf{s}(x + x', t)]\, dx' \tag{2.4.14a}$$

$$= \int_0^\infty \kappa(x')[\mathbf{g}(\mathbf{x}(x,t)) - \mathbf{g}(\mathbf{x}(x + x', t))]\, dx'. \tag{2.4.14b}$$

As examples, consider the control forces given by (2.4.12a) and (2.4.13a). In the first case, the kernel is a δ-function which is shifted by Δx, i.e., $\kappa(x') = \delta(x' + \Delta x)$. In the latter case, the kernel consists similarly of two δ-functions: $\kappa(x') = \delta(x' + \Delta x) + \delta(x' - \Delta x)$.

The integral kernel provides information of the structure, e.g., the symmetry, of the spatial coupling. If, for instance, a rotational symmetry is present in the coupling of a two-dimensional system, the control force is given by

$$\begin{aligned}\mathbf{F}(x,y,t) &= \int_0^{2\pi}\int_0^\infty \kappa(r)[\mathbf{s}(x,y,t) - \mathbf{s}(x + r\cos\varphi, y + r\sin\varphi, t)]\, dr d\varphi \\ &= \int_0^{2\pi}\int_0^\infty \kappa(r)[\mathbf{g}(\mathbf{x}(x,y,t)) - \mathbf{g}(\mathbf{x}(x + r\cos\varphi, y + r\sin\varphi, t))]\, dr d\varphi,\end{aligned} \tag{2.4.15}$$

where r and φ denote the polar coordinates and the kernel $\kappa(r)$ depends only on the radius $r = \sqrt{x^2 + y^2}$. If the kernel exhibits a minimum at $r_0 > 0$, the coupling is known as Mexican-hat potential which occurs, for instance, in the context of neural models realized as a two-dimensional reaction-diffusion system [78, 80]. In this context, the terminology Mexican-hat refers to the shape of the local connectivity network in the cortical tissue.

It is of course possible to combine all above mentioned extensions. For instance, additional filter in the feedback scheme can result in a non-zero control loop latency which arise from the time needed to constructs the filtered signal. In the framework of spatio-temporal dynamics, space delays and time delays can be mixed since nonlocal signals can be time-delayed [78].

To conclude this section, I will discuss an extension to an adaptive feedback controller to find a value of the feedback gain which yields successful stabilization [5]. The basic idea is to regard the feedback gain K as an additional dynamic variable. Therefore, one more differential equation must be added to the system to

account for the temporal dynamics of K. In order to derive this additional equation, one can consider a state-dependent goal or error function Q given by [81]

$$Q(x(t), x(t-\tau)) = \frac{1}{2}[x(t) - x(t-\tau)]^2, \tag{2.4.16}$$

which vanishes if the system is stabilized. Substituting the right-hand side of the system's equation with control into the time derivative of Q yields the desired equation by the following relation

$$\frac{d}{dt}K(t) = -\gamma \frac{\partial}{\partial K}\left(\frac{dQ}{dt}\right), \tag{2.4.17}$$

where the parameter $\gamma > 0$ denotes the adaptation gain. For details see Ref. [81]. It has been shown that unstable steady states of focus type can be stabilized by this method which automatically chooses a suitable value for the feedback gain [81]. The adaptive control scheme can also be used to track periodic orbits in chaotic systems [24, 82].

The proposed adaptive algorithm is also known as gradient method [83–85]. A similar algorithm was used for adaptive synchronization of chaotic systems [86] and the control of a steady state in the Lorenz system by proportional control [87].

2.5 Linear Stability Analysis

In this section, I will elaborate the concept of linear stability analysis for systems subject to time-delayed feedback which will lead to a so-called characteristic equations. This technique will be used several times in the subsequent chapters.

Consider a small deviation $\delta\mathbf{x}(t)$ from a target state $\mathbf{x}^*(t)$, e.g., a steady state or a periodic orbit: $\delta\mathbf{x}(t) = \mathbf{x}(t) - \mathbf{x}^*(t)$. A linearization of the system equation including time-delayed feedback as given in (2.1.2) yields up to linear order in $\delta\mathbf{x}(t)$

$$\frac{d}{dt}\mathbf{x}(t) = \mathbf{f}(\mathbf{x}(t)) - \mathbf{h}[K\{\mathbf{g}(\mathbf{x}(t)) - \mathbf{g}(\mathbf{x}(t-\tau))\}] \tag{2.5.1a}$$

$$\begin{aligned} &= \mathbf{f}(\mathbf{x}^*(t)) - \mathbf{h}[K\{\mathbf{g}(\mathbf{x}^*(t)) - \mathbf{g}(\mathbf{x}^*(t-\tau))\}] \\ &\quad + \underbrace{\frac{\partial \mathbf{f}(\mathbf{x}(t))}{\partial \mathbf{x}(t)}\bigg|_{\mathbf{x}(t)=\mathbf{x}^*(t)}}_{\mathrm{I}}[\mathbf{x}(t) - \mathbf{x}^*(t)] \\ &\quad - \underbrace{\frac{\partial \mathbf{h}[K\mathbf{g}(\mathbf{x}(t))]}{\partial K\mathbf{g}(\mathbf{x}(t))}\frac{\partial K\mathbf{g}(\mathbf{x}(t))}{\partial \mathbf{x}(t)}\bigg|_{\mathbf{x}(t)=\mathbf{x}^*(t)}}_{\mathrm{II}}[\mathbf{x}(t) - \mathbf{x}^*(t)] \\ &\quad + \overbrace{\frac{\partial \mathbf{h}[K\mathbf{g}(\mathbf{x}(t))]}{\partial K\mathbf{g}(\mathbf{x}(t))}\frac{\partial K\mathbf{g}(\mathbf{x}(t))}{\partial \mathbf{x}(t)}\bigg|_{\mathbf{x}(t)=\mathbf{x}^*(t)}}[\mathbf{x}(t-\tau) - \mathbf{x}^*(t-\tau)]. \end{aligned} \tag{2.5.1b}$$

The first term $\mathbf{f}(\mathbf{x}^*(t))$ gives the derivative of the invariant solution $\mathbf{x}^*(t)$. The second term vanishes due to the noninvasive property of the control scheme. The term labelled as *I* represents the Jacobian matrix of $\mathbf{f}$ evaluated at $\mathbf{x}^*(t)$ and the matrix *II* can be abbreviated as $\mathbf{B}(t)$ summarizing the linearized control terms. This leads to an equivalent expression

$$\frac{d}{dt}\delta\mathbf{x}(t) = \mathbf{A}(t)\delta\mathbf{x}(t) - \mathbf{B}(t)[\delta\mathbf{x}(t) - \delta\mathbf{x}(t-\tau)], \tag{2.5.2}$$

where $\mathbf{A}(t)$ denotes the Jacobian matrix of the uncontrolled system. If the target state is a fixed point, i.e., $\mathbf{x}(t) \equiv \mathbf{x}^*$, the matrices $\mathbf{A}$ and $\mathbf{B}$ are time independent. Thus, an exponential ansatz for $\delta\mathbf{x}$ leads to a characteristic equation whose roots determine the stability.

If the linear stability analysis is performed at a periodic orbit with period τ, i.e., $\mathbf{x}(t) = \mathbf{x}^*(t) = \mathbf{x}^*(t-\tau)$, both matrices are periodic with that same period and Floquet theory will guarantees that solutions $\delta\mathbf{x}(t)$ of (2.5.2) can be decomposed into Floquet modes

$$\delta\mathbf{x}(t) = \sum_{j=0}^{\infty} c_j e^{\Lambda_j t}\mathbf{u}_j(t), \tag{2.5.3}$$

where $\mathbf{u}_j(t)$ and Λ_j denote the *j*th Floquet mode and corresponding complex Floquet exponent, respectively [12, 28, 45, 46, 61, 88–91]. Note that the Floquet modes are periodic with period τ, i.e., $\mathbf{u}_j(t) = \mathbf{u}_j(t+\tau)$. Inserting this decomposition into (2.5.2) yields

$$\Lambda\mathbf{u}(t) + \frac{d}{dt}\mathbf{u}(t) = \mathbf{A}(t)\mathbf{u}(t) - \mathbf{B}(t)\left[\mathbf{u}(t) - e^{-\Lambda\tau}\mathbf{u}(t-\tau)\right] \tag{2.5.4a}$$

$$= \mathbf{A}(t)\mathbf{u}(t) - \mathbf{B}(t)\left(1 - e^{-\Lambda\tau}\right)\mathbf{u}(t), \tag{2.5.4b}$$

where the subscript *j* is omitted for notational convenience. Finally, one arrives at a differential equation for $\mathbf{u}(t)$

$$\frac{d}{dt}\mathbf{u}(t) = \left[\mathbf{A}(t) - \mathbf{B}(t)\left(1 - e^{-\Lambda\tau}\right) - \Lambda\mathbf{Id}\right]\mathbf{u}(t) \tag{2.5.5}$$

with the $n \times n$ identity matrix $\mathbf{Id}$.

Using the fundamental matrix $\Phi(t)$ determined by the differential equation

$$\frac{d}{dt}\Phi(t) = [\mathbf{A}(t) - \mathbf{B}(t)]\Phi(t) \tag{2.5.6}$$

with $\Phi(0) = \mathbf{Id}$, one can write the solutions of (2.5.2) as $\delta\mathbf{x}(t) = \Phi(t)\mathbf{x}_{\text{init}}$ with some initial condition $\mathbf{x}_{\text{init}}$.

The spectrum of the Floquet exponents is given by the roots of the characteristic equation

$$\det\left[\mathbf{A}(t) - \mathbf{B}(t)\left(1 - e^{-\Lambda\tau}\right) - \Lambda\mathbf{Id}\right] = 0. \tag{2.5.7}$$

Note that a similar equation can be derived in the context of steady states $\mathbf{x}^*$ where an ansatz for $\delta\mathbf{x}(t)$ is given by $\delta\mathbf{x}(t) = e^{\Lambda t}\mathbf{x}_{\text{init}}$. Then, (2.5.7) describes a characteristic equation for the eigenvalues Λ of the controlled system.

The control scheme is successful if the real parts of all Floquet exponents or, in case of steady states, all eigenvalues are negative. An equivalent statement is that all multipliers μ defined as $\mu = \exp(\Lambda\tau)$ are located inside the unit circle in the complex plane. This Floquet multiplier can be understood as the rate how the distance from the invariant solution increases in an interval $[t, t + \tau]$.

In the case of extended time-delayed feedback as given by (2.2.1), the infinite series in the control force collapses as a geometric series

$$\mathbf{F}(t) = \sum_{n=0}^{\infty} R^n[\mathbf{s}(t - n\tau) - \mathbf{s}(t - (n+1)\tau)] \tag{2.5.8a}$$

$$= \sum_{n=0}^{\infty} R^n\left[e^{\Lambda(t-n\tau)}\mathbf{u}(t - n\tau) - e^{\Lambda[t-(n+1)\tau]}\mathbf{u}(t - (n+1)\tau)\right] \tag{2.5.8b}$$

$$= e^{\Lambda t}\left(1 - e^{-\Lambda\tau}\right)\sum_{n=0}^{\infty} R^n e^{-n\Lambda\tau}\mathbf{u}(t) \tag{2.5.8c}$$

$$= e^{\Lambda t}\frac{1 - e^{-\Lambda\tau}}{1 - Re^{-\Lambda\tau}}\mathbf{u}(t). \tag{2.5.8d}$$

Therefore, the characteristic equation in the case of extended time-delayed feedback control reads

$$\det\left[\mathbf{A}(t) - \mathbf{B}(t)\frac{1 - e^{-\Lambda\tau}}{1 - Re^{-\Lambda\tau}} - \Lambda\mathbf{Id}\right] = 0. \tag{2.5.9}$$

The following chapters will specify the matrices $\mathbf{A}$ and $\mathbf{B}$ such that (2.5.7) and (2.5.9) become a powerful tool for the stability analysis of the target state. In the case of phase-dependent coupling or additional latency as mentioned in Sect. 2.4, a characteristic equation can be derived as well. Details of the corresponding derivations will be discussed in Sects. 3.5 and 3.4.

2.6 Transfer Function

In this section, I will discuss effects of time-delayed feedback control in the frequency domain and I will show how the different frequencies in the control signal contribute to the control force. The transform into Fourier space is especially helpful if additional filters are present in the feedback loop. I will discuss

both low-pass and bandpass filters and show how these filters influence the control signal in the formalism of transfer functions.

The transfer function of the extended time-delayed control scheme is derived in the following [34]. Starting from the definition of the control force $\mathbf{F}(t)$ given by (2.2.1a), the transfer function can be calculated by a Fourier transform

$$\mathbf{F}(t) = \sum_{n=0}^{\infty} R^n [\mathbf{s}(t - n\tau) - \mathbf{s}(t - (n+1)\tau)] \tag{2.6.1a}$$

$$\Rightarrow \hat{\mathbf{F}}(\omega) = \int_{-\infty}^{\infty} dt\, e^{-i\omega t} \sum_{n=0}^{\infty} R^n [\mathbf{s}(t - n\tau) - \mathbf{s}(t - (n+1)\tau)] \tag{2.6.1b}$$

$$= \sum_{n=0}^{\infty} R^n \left[e^{-in\omega\tau} \hat{\mathbf{s}}(\omega) - e^{-i(n+1)\omega\tau} \hat{\mathbf{s}}(\omega) \right] \tag{2.6.1c}$$

$$= \sum_{n=0}^{\infty} R^n e^{-in\omega\tau} (1 - e^{-i\omega\tau}) \hat{\mathbf{s}}(\omega). \tag{2.6.1d}$$

Using the geometric series

$$\sum_{n=0}^{\infty} R^n \left(e^{-i\omega\tau}\right)^n = \frac{1}{1 - Re^{-i\omega\tau}} \tag{2.6.2}$$

yields the Fourier transform $\hat{\mathbf{F}}(\omega)$ of the extended time-delayed control force

$$\hat{\mathbf{F}}(\omega) = T_1(\omega) \hat{s}(\omega), \tag{2.6.3}$$

where the transfer function $T_1(\omega)$ is given by

$$T_1(\omega) = \frac{1 - e^{-i\omega\tau}}{1 - Re^{-i\omega\tau}}. \tag{2.6.4}$$

Figure 2.2 depicts the absolute value of this transfer function $|T_1(\omega)|$ for different values of the memory parameter $R = 0$, 0.3, 0.6, and 0.9 as black (solid), (dashed), green (dotted), and blue (dash-dotted) curves, respectively. As discussed in Ref. [34] in the context of stabilization of periodic orbits, the transfer function drops to zero at multiples of the basic frequency τ^{-1}. In the context of stabilization of periodic orbits, this frequency belongs to the periodic orbit under control to guarantee the noninvasiveness of time-delayed feedback. One can see that the notches at these frequencies become narrower as R increases. Due to the notches, the frequency of the periodic orbit does not contribute to the control signal, so that the control force vanishes if stabilization is successful. The steeper notches for larger R indicate that the extended time-delayed feedback is more sensitive to frequencies different from the one to be controlled, so that more feedback is produced for these unwanted frequencies, which makes the control scheme more efficient.

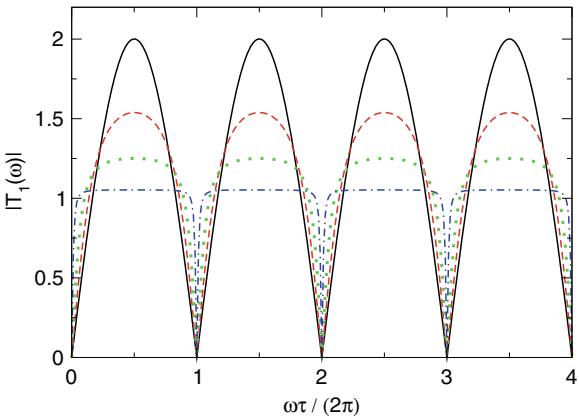

Fig. 2.2 Absolute value of the transfer function of the extended time-delayed feedback scheme according to (2.6.4). The *black* (*solid*), *red* (*dashed*), *green* (*dotted*), and *blue* (*dash-dotted*) curves correspond to different memory parameters $R = 0$, 0.3, 0.6, and 0.9, respectively

The maximum value of the transfer function $|T_1(\omega)|$ approaches 1 for R closer to 1 and the plateaus become flatter. Therefore, intermediate frequencies generate a smaller response for larger R and thus are less likely to destabilize the system. The frequency comb shown in Fig. 2.2 can be realized experimentally for the stabilization of *cw* emission and intensity pulsations of a semiconductor laser via an all-optical feedback [30, 31, 92]. The feedback is implemented by a Fabry–Perrot interferometer attached to the laser.

As mentioned in Sect. 2.4, there is a variety of extensions of the original time-delayed feedback scheme. For example, it is desirable to include filter in the control loop in order to avoid unwanted frequencies. This filtered feedback has been successfully implemented in optical experiments [64, 65, 67, 93–99] as well as in nonlinear electronic circuits [33, 100], charge transport in semiconductor devices [13, 14, 49], and for the control of unstable steady states of focus type [10, 57, 58].

In the following, I will derive the transfer function of a low-pass filter. Then I will show that a combination of a low-pass filter and time-delayed feedback can be treated in the Fourier space by product of the respective transfer functions.

Similar to the derivation of (2.6.4), the transfer function of the low-pass filter is given by the Fourier transform of (2.4.4)

$$\overline{\mathbf{s}}(t) = \alpha \int_{-\infty}^{t} \mathbf{s}(t') e^{-\alpha(t-t')}\, dt' \tag{2.6.5a}$$

$$\Rightarrow \hat{\overline{\mathbf{s}}}(\omega) = \int_{-\infty}^{\infty} e^{-i\omega t} \alpha \int_{-\infty}^{t} \mathbf{s}(t') e^{-\alpha(t-t')}\, dt' dt. \tag{2.6.5b}$$

The second integral of the right-hand side of (2.6.5b) is a convolution of the form

$$f_1(t) * f_2(t) = \int_{-\infty}^{\infty} f_1(\tau) f_2(t-\tau)\, d\tau, \tag{2.6.6}$$

where the functions $f_1(t)$ and $f_2(t)$ are given in the present case by

$$f_1(t) = \mathbf{s}(t) \qquad \text{and} \qquad f_2(t) = \begin{cases} \alpha e^{-\alpha t}, & t \geq 0 \\ 0, & t < 0 \end{cases}. \tag{2.6.7}$$

With these definitions, (2.6.6) becomes

$$f_1(t) * f_2(t) = \alpha \int_{-\infty}^{t} \mathbf{s}(t') e^{-\alpha(t-t')}\, dt'. \tag{2.6.8}$$

Fourier theory yields that the Fourier transform of a convolution of two functions is the product of the single transformed functions

$$\mathcal{F}[f_1(t) * f_2(t)] = \mathcal{F}[f_1(t)]\mathcal{F}[f_2(t)]. \tag{2.6.9}$$

Therefore the Fourier transform of the low-pass filter is given by

$$\hat{\bar{\mathbf{s}}}(\omega) = \mathcal{F}[\mathbf{s}(t)]\mathcal{F}[f_2(t)] \tag{2.6.10a}$$

$$= \hat{\mathbf{s}}(\omega) \underbrace{\int_{-\infty}^{\infty} f_2(t) e^{-i\omega t}\, dt}_{\alpha \int_0^{\infty} e^{-\alpha t} e^{-i\omega t}\, dt} \tag{2.6.10b}$$

$$= \alpha \hat{\mathbf{s}}(\omega) \left[\frac{1}{-\alpha - i\omega} e^{-(\alpha + i\omega)t} \right]_0^{\infty} \tag{2.6.10c}$$

$$= \hat{\mathbf{s}}(\omega) \frac{1}{1 + i\frac{\omega}{\alpha}}. \tag{2.6.10d}$$

The last equation can be rewritten introducing the transfer function of the low-pass filter $T_2(\omega)$

$$\bar{\mathbf{s}}(\omega) = \frac{1}{1 + i\frac{\omega}{\alpha}} \mathbf{s}(\omega) = T_2(\omega)\mathbf{s}(\omega). \tag{2.6.11}$$

Figure 2.3 shows the frequency dependence of the absolute value of the transfer function $|T_2(\omega)|$ of the low-pass filter for different values of the cutoff frequency α. The black (solid), red (dashed), green (dotted), and blue (dash-dotted) curves refer to different values of $\alpha\tau = 0.25$, 0.5, 0.75, and 1, respectively. It can be seen that the absolute value of the transfer function is

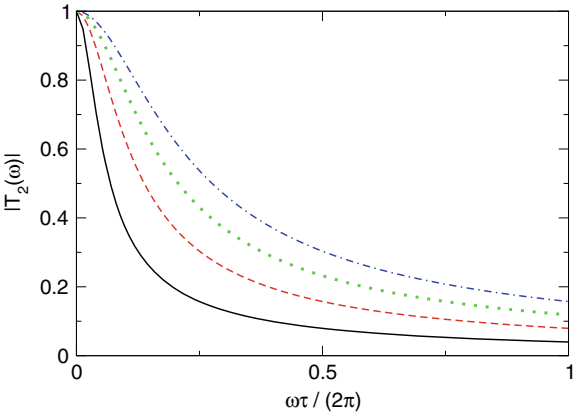

Fig. 2.3 Absolute value of the transfer function of the low-pass filter according to (2.6.11). The *black* (*solid*), *red* (*dashed*), *green* (*dotted*), and *blue* (*dash-dotted*) curves correspond to different values of the cutoff frequency $\alpha\tau = 0.25$, 0.5, 0.75, and 1, respectively

strictly monotonic decreasing. Hence, high frequencies are suppressed. For instance, the amplitude of the frequency at $\omega = \alpha$ is reduced by a factor of $1/\sqrt{2}$. Therefore α is called a cutoff frequency. One can see that larger values of α lead to a slower decrease of the transfer function. Thus higher frequencies can pass the filter to a larger extent.

Consider now the combination of the extended time-delayed control scheme and the low-pass filter. In this case the feedback of (2.2.1a) is given by

$$\mathbf{F}(t) = \sum_{n=0}^{\infty} R^n[\bar{\mathbf{s}}(t - n\tau) - \bar{\mathbf{s}}(t - (n+1)\tau)], \tag{2.6.12}$$

where $\bar{\mathbf{s}}(t)$ denotes again the low-pass filtered version of the control signal $\mathbf{s}(t)$ according to (2.4.4). A Fourier transform of (2.6.12) yields similar to the derivation of (2.6.3)

$$\hat{\mathbf{F}}(\omega) = \sum_{n=0}^{\infty} R^n e^{-in\omega\tau}(1 - e^{-i\omega\tau})\hat{\bar{\mathbf{s}}}(\omega) \tag{2.6.13a}$$

$$= \frac{1 - e^{-i\omega\tau}}{1 - Re^{-i\omega\tau}}\hat{\bar{\mathbf{s}}}(\omega). \tag{2.6.13b}$$

Using the notation of transfer functions, the last equation can be rewritten using (2.6.11)

$$\hat{\mathbf{F}}(\omega) = T_1(\omega)\hat{\bar{\mathbf{s}}}(\omega) \tag{2.6.14a}$$

$$= T_1(\omega)T_2(\omega)\hat{\mathbf{s}}(\omega) \tag{2.6.14b}$$

$$= T(\omega)\hat{\mathbf{s}}(\omega), \tag{2.6.14c}$$

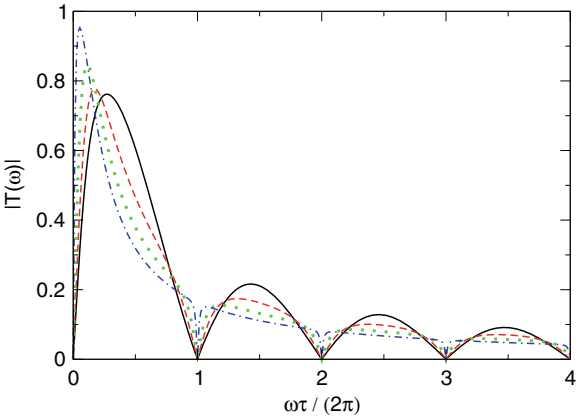

Fig. 2.4 Absolute value of the transfer function of the extended time-delayed feedback method combined with low-pass filtering according to (2.6.15). The *black* (*solid*), *red* (*dashed*), *green* (*dotted*), and *blue* (*dash-dotted*) curves correspond to different memory parameters $R = 0$, 0.3, 0.6, and 0.9, respectively. The cutoff frequency is fixed at $\alpha\tau = 1$

where the combined transfer function $T(\omega)$ is given by

$$T(\omega) = \frac{1 - e^{-i\omega\tau}}{1 - Re^{-i\omega\tau}} \frac{1}{1 + i\frac{\omega}{\alpha}}. \tag{2.6.15}$$

Note that the combined transfer function $T(\omega)$ is the product of the single functions for the extended time-delayed feedback $T_1(\omega)$ and the low-pass filter $T_2(\omega)$.

The absolute value of $|T(\omega)|$ is displayed in Fig. 2.4 for different memory parameters R and fixed cutoff frequency $\alpha\tau = 1$, where the black (solid), red (dashed), green (dotted), and blue (dash-dotted) curves refer to $R = 0$, 0.3, 0.6, and 0.9, respectively. As in Fig. 2.2, there are notches at multiples of the basic frequency τ^{-1} because the roots of $|T_1(\omega)|$ persist. The amplitudes of frequencies larger than the cutoff frequency α are reduced and thus are only minor contributions to the feedback response. This is important to notice in order to understand how the low-pass filter improves the controllability of the system as will be discussed in the following.

In the context of time-delayed feedback applied to the nonlinear electron transport in semiconductor devices like a superlattice [29, 101, 102], additional low-pass filtering has been successfully used to suppress chaotic current oscillations and to stabilize a periodic orbit [13, 48, 49]. This is not possible without the filter, because the unfiltered feedback scheme includes unwanted high frequencies which arise from well-to-well hopping of the electrons. As a consequence, the control scheme can stabilize the unwanted frequencies instead of the frequency of the target orbit. A low-pass filter given by (2.4.4) and (2.6.11) with an appropriate cutoff frequency eliminates these frequency components in the control signal.

Similar to a low-pass filter it is also possible to suppress low frequencies, which can be realized ba a high-pass filter, or include only an intermediate range of frequencies to enter the control force. The latter can be implemented by a bandpass

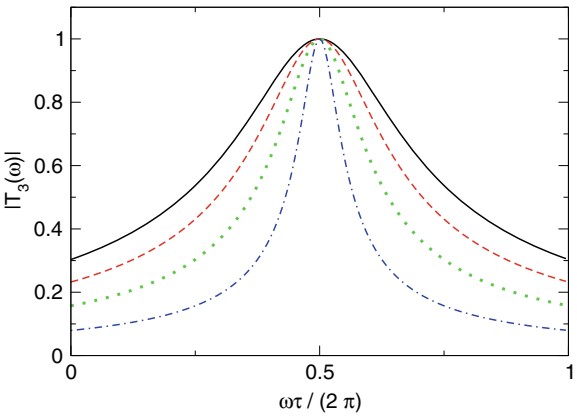

Fig. 2.5 Absolute value of the transfer function of the bandpass filter according to (2.6.16). The *black* (*solid*), *red* (*dashed*), *green* (*dotted*), and *blue* (*dash-dotted*) curves correspond to different values of $\alpha\tau = 0.25$, 0.5, 0.75, and 1, respectively. The frequency shift is fixed at $\omega_0\tau = \pi$

filter. The transfer function $T_3(\omega)$ is this device is given by a frequency shift ω_0 added to the low-pass filter $T_2(\omega)$. This yields

$$T_3(\omega) = \frac{1}{1 + i\frac{\omega - \omega_0}{\alpha}} \tag{2.6.16}$$

and the bandpass filter signal becomes

$$\hat{\bar{\mathbf{s}}}(\omega) = T_3(\omega)\hat{\mathbf{s}}(\omega). \tag{2.6.17}$$

Note that vanishing ω_0 recovers the low-pass filter. The equivalent differential equation reads

$$\frac{d}{dt}\bar{\mathbf{s}}(t) = -\alpha\bar{\mathbf{s}}(t) + \alpha\mathbf{s}(t) + i\omega_0\mathbf{s}(t). \tag{2.6.18}$$

Compare with the equation for the low-pass filter given by (2.4.3).

Figure 2.5 depicts the absolute value of the transfer function of the bandpass filter $|T_3(\omega)|$ for different values of $\alpha\tau = 0.25$, 0.5, 0.75, and 1 as black (solid), red (dashed), green (dotted), and blue (dash-dotted) curves, respectively. The frequency shift is fixed at $\omega_0\tau = \pi$. In analogy to the combination of low-pass filtering and time-delayed feedback, one could include a bandpass filter in the delay line. In Fourier space, this leads again the product of the respective transfer functions.

The extension of bandpass filtering in the control loop has been used to investigate a Hopf bifurcation in an experiment with a nonlinear electronic circuit including band-limited feedback [33, 100]. A bandpass filter has also a large relevance in optical systems. Filtered optical feedback has been used for both experimental and theoretical investigation of *cw* emission, frequency and relaxation oscillations in semiconductor lasers [64, 65, 67, 94, 97, 98]. These devices provide an interest experimental system since they exhibit a rich bifurcation

scenario [93, 96, 103–106]. In this context, the complex electric field can be chosen as control signal **s** which is altered by the filter [58].

2.7 Intermediate Conclusion

In this chapter, I have introduced time-delayed feedback control. This feedback scheme generates a control signal from the difference $s(t) - s(t - \tau)$ between the present and an earlier value of an appropriate system variable s. It is noninvasive since the control forces vanish if the target state which could be, for instance, a periodic orbit or a steady state is reached. Due to this property, the unstable states themselves of the original system are not changed by the control, but only their neighborhood is adjusted such that neighboring trajectories converge to it, i.e., the control forces act only if the system deviates from the state to be stabilized. Involving no numerically expensive computations and applicable in experimental setups, time-delayed feedback control is capable of controlling systems with very fast dynamics still in real-time mode [30, 32, 35]. Moreover, detailed knowledge of the target state is not required.

In addition, I have discussed various modifications of the original control scheme such as multiple time-delayed feedback, control loop latency, filtering of the control signal, or nonlocal coupling with spatial delays. Furthermore, I have considered different realizations in terms of coupling functions which measure the system's variables for construction of the control signal and which specify the application of the control force back to the system. Towards the end of this chapter, I applied the concept of transfer functions to the control scheme which added an additional perspective and opened connections with experimental realizations.

This chapter will serve as central node connecting all subsequent chapters where I will apply the time-delayed feedback method to a variety of different dynamic systems. The next chapter will be devoted to the control of steady states. I will also consider next to the original Pyragas scheme many of the above-mentioned modifications which are experimentally relevant. In Chaps. 4–6, I will then discuss other classes of dynamic systems such as periodic states, neutral delay-differential equations, and excitable systems.

References

1. Ott E, Grebogi C, Yorke JA (1990) Controlling chaos. Phys Rev Lett 64:1196
2. Nijmeijer H, Schaft AVD (1996) Nonlinear dynamical control systems, 3rd edn. Springer, New York
3. Ogata K (1997) Modern control engineering. Prentice-Hall, New York.
4. Fradkov AL, Pogromsky AY (1998) Introduction to control of oscillations and chaos. World Scientific, Singapore

5. Fradkov AL, Miroshnik IV, Nikiforov VO (1999). Nonlinear and adaptive control of complex systems. Kluwer, Dordrecht
6. Schuster HG (Editor) (1999) Handbook of chaos control. Wiley-VCH, Weinheim
7. Schöll E, Schuster HG (eds) (2008) Handbook of chaos control. Wiley-VCH, Weinheim. Second completely revised and enlarged edition
8. Pyragas K (1992) Continuous control of chaos by self-controlling feedback. Phys Lett A 170:421
9. Socolar JES, Sukow DW, Gauthier DJ (1994) Stabilizing unstable periodic orbits in fast dynamical systems. Phys Rev E 50:3245
10. Hövel P, Schöll E (2005) Control of unstable steady states by time-delayed feedback methods. Phys Rev E 72:046203
11. Sieber J, Krauskopf B (2007) Control based bifurcation analysis for experiments. Nonlinear Dyn 51:365
12. Schlesner J (2002) Nichtlineare Oszillationen in Halbleiterübergittern unter zeitverzögerter Rückkopplung. Master's thesis, Technische Universität Berlin
13. Schlesner J, Amann A, Janson NB, Just W, Schöll E (2003) Self-stabilization of high frequency oscillations in semiconductor superlattices by time-delay autosynchronization. Phys Rev E 68:066208
14. Schlesner J, Amann A, Janson NB, Just W, Schöll E (2004) Self-stabilization of chaotic domain oscillations in superlattices by time-delayed feedback control. Semicond Sci Technol 19:S34
15. Kehrt M (2008) Zeitverzögerte Rückkopplungskontrolle eines global gekoppelten Reaktions-Diffusions-Modells. Master's thesis, Technische Universität Berlin
16. Hunt BR, Ott E (1996) Optimal periodic orbits of chaotic systems. Phys Rev Lett 76:2254
17. Hunt BR, Ott E (1996) Optimal periodic orbits of chaotic systems occur at low period. Phys Rev E 54:328
18. Yang T-H, Hunt BR, Ott E (2000) Optimal periodic orbits of continuous time chaotic systems. Phys Rev E 62:1950
19. Zoldi SM, Greenside HS (1998) Comment on optimal periodic orbits of chaotic systems. Phys Rev Lett 80:1790
20. Hunt BR, Ott E (1998) Hunt and Ott reply. Phys Rev Lett 80:1791
21. Just W, Reckwerth D, Möckel J, Reibold E, Benner H (1998) Delayed feedback control of periodic orbits in autonomous systems. Phys Rev Lett 81:562
22. Franceschini G, Bose S, Schöll E (1999) Control of chaotic spatiotemporal spiking by time-delay autosynchronisation. Phys Rev E 60:5426
23. Zoldi SM, Franceschini G, Bose S, Schöll E (2000) Stabilizing unstable periodic orbits in reaction-diffusion systems by global time-delayed feedback control. In: Fiedler B, Gröger K, Sprekels J (eds) Proceedings of Equadiff 99. World Scientific Publishing, Singapore, p 1311
24. Yu X (1999) Tracking inherent periodic orbits in chaotic dynamic systems via adaptive variable structure time-delay self control. IEEE Trans Circuits Syst 46:1408
25. Ando H, Boccaletti S, Aihara K (2007) Automatic control and tracking of periodic orbits in chaotic systems. Phys Rev E 75:066211
26. Pyragas K, Pyragas V, Kiss IZ, Hudson JL (2002) Stabilizing and tracking unknown steady states of dynamical systems. Phys Rev Lett 89:244103
27. Parmananda P (2003) Tracking fixed-point dynamics in an electrochemical system using delayed-feedback control. Phys Rev E 67:045202(R)
28. Unkelbach J, Amann A, Just W, Schöll E (2003) Time–delay autosynchronization of the spatiotemporal dynamics in resonant tunneling diodes. Phys Rev E 68:026204
29. Schöll E (2004) Pattern formation in semiconductors: control of spatio-temporal dynamics. Ann Phys (Leipzig) 13:403. Special Topic Issue, edited by Friedrich R, Kuhn T, Linz S
30. Schikora S, Hövel P, Wünsche HJ, Schöll E, Henneberger F (2006) All-optical noninvasive control of unstable steady states in a semiconductor laser. Phys Rev Lett 97:213902

31. Schikora S, Wünsche HJ, Henneberger F (2008) All-optical noninvasive chaos control of a semiconductor laser. Phys Rev E 78:025202
32. Blakely JN, Illing L, Gauthier DJ (2004) Controlling fast chaos in delay dynamical systems. Phys Rev Lett 92:193901
33. Illing L, Gauthier DJ (2005) Hopf bifurcations in time-delay systems with band-limited feedback. Physica D 210:180
34. Sukow DW, Bleich ME, Gauthier DJ, Socolar JES (1997) Controlling chaos in a fast diode resonator using time-delay autosynchronisation: experimental observations and theoretical analysis. Chaos 7:560
35. Gauthier DJ, Sukow DW, Concannon HM, Socolar JES (1994) Stabilizing unstable periodic orbits in a fast diode resonator using continuous time-delay autosynchronization. Phys Rev E 50:2343
36. Bleich ME, Socolar JES (1996) Stability of periodic orbits controlled by time-delay feedback. Phys Lett A 210:87
37. Bleich ME, Socolar JES (1996) Controlling spatiotemporal dynamics with time-delay feedback. Phys Rev E 54:R17
38. Schneider FM, Schöll E, Dahlem MA (2009) Controlling the onset of traveling pulses in excitable media by nonlocal spatial coupling and time delayed feedback. Chaos 19:015110
39. Hövel P, Shah SA, Dahlem MA, Schöll E (2009) Feedback-dependent control of stochastic synchronization in coupled neural systems. In: Fortuna L, Frasca M (eds) Proceedings of 4th international scientific conference on physics and control (PhysCon 09). IPACS Open Access Library http://lib.physcon.ru (e-Library of the International Physics and Control Society), http://arxiv.org/abs/0911.2334v1
40. Yeung MKS, Strogatz SH. (1999) Time delay in the Kuramoto model of coupled oscillators. Phys Rev Lett 82:648
41. Lysyansky B, Maistrenko Y, Tass PA (2008) Coexistence of numerous synchronized and desynchronized states in a model of two phase oscillators coupled with delay. Int J Bifur Chaos 18:1791
42. Rosenblum MG, Pikovsky AS (2004) Controlling synchronization in an ensemble of globally coupled oscillators. Phys Rev Lett 92:114102
43. Popovych OV, Hauptmann C, Tass PA (2005) Effective desynchronization by nonlinear delayed feedback. Phys Rev Lett 94:164102
44. Popovych OV, Hauptmann C, Tass PA (2005) Demand-controlled desynchronization of brain rhythms by means of nonlinear delayed feedback. In: Proceedings of IEEE Engineering and Medicine Biology. 27th Annual conference
45. Beck O, Amann A, Schöll E, Socolar JES, Just W (2002) Comparison of time-delayed feedback schemes for spatio-temporal control of chaos in a reaction-diffusion system with global coupling. Phys Rev E 66:016213
46. Baba N, Amann A, Schöll E, Just W (2002) Giant improvement of time-delayed feedback control by spatio-temporal filtering. Phys Rev Lett 89:074101
47. Just W, Popovich S, Amann A, Baba N, Schöll E (2003) Improvement of time–delayed feedback control by periodic modulation: analytical theory of Floquet mode control scheme. Phys Rev E 67:026222
48. Hövel P (2004) Effects of chaos control and latency in time-delay feedback methods. Master's thesis, Technische Universität Berlin
49. Schöll E, Hizanidis J, Hövel P, Stegemann G (2007) Pattern formation in semiconductors under the influence of time-delayed feedback control and noise. In: Schimansky-Geier L, Fiedler B, Kurths J, Schöll E (eds) Analysis and control of complex nonlinear processes in physics, chemistry and biology. World Scientific, Singapore, pp 135–183
50. Stegemann G, Balanov AG, Schöll E (2006) Delayed feedback control of stochastic spatiotemporal dynamics in a resonant tunneling diode. Phys Rev E 73:016203
51. Stegemann G, Schöll E (2007) Two-dimensional spatiotemporal pattern formation in the double-barrier resonant tunneling diode. New J Phys 9:55

52. Hizanidis J, Balanov AG, Amann A, Schöll E (2006) Noise-induced oscillations and their control in semiconductor superlattices. Int J Bifur Chaos 16:1701
53. Hizanidis J, Balanov AG, Amann A, Schöll E (2005) Control of noise-induced oscillations in superlattices by delayed feedback. In: Gonzales T, Mateos J, Pardo D (eds) Proceedings of 18th international conference on noise and fluctuations (ICNF-2005), vol 780. American Institute of Physics, Melville, New York), pp 41–44. ISBN 0-7354-0267-1
54. Hizanidis J, Schöll E (2008) Control of noise-induced spatiotemporal patterns in superlattices. Phys Stat Sol (c) 5:207
55. Hizanidis J (2008) Control of noise-induced spatio-temporal dynamics in superlattices. Ph.D. thesis, Technische Universität Berlin
56. Kehrt M, Hövel P, Flunkert V, Dahlem MA, Rodin P, Schöll E (2009) Stabilization of complex spatio-temporal dynamics near a subcritical Hopf bifurcation by time-delayed feedback. Eur Phys J B 68:557
57. Dahms T, Hövel P, Schöll E (2007) Control of unstable steady states by extended time-delayed feedback. Phys Rev E 76:056201
58. Dahms T, Hövel P, Schöll E (2008) Stabilizing continuous-wave output in semiconductor lasers by time-delayed feedback. Phys Rev E 78:056213
59. Balanov AG, Janson NB, Schöll E (2005) Delayed feedback control of chaos: bifurcation analysis. Phys Rev E 71:016222
60. Just W, Reckwerth D, Reibold E, Benner H (1999) Influence of control loop latency on time-delayed feedback control. Phys Rev E 59:2826
61. Hövel P, Socolar JES (2003) Stability domains for time-delay feedback control with latency. Phys Rev E 68:036206
62. Manor Y, Koch C, Segev I (1991) Effect of geometrical irregularities on propagation delay in axonal trees. Biophys J 60: 1424
63. Schwark HD, Jones EG (1989) The distribution of intrinsic cortical axons in area 3b of cat primary somatosensory cortex. Exp Brain Res 78:501
64. Yousefi M, Lenstra D (1999) Dynamical behavior of a semiconductor laser with filtered external optical feedback. IEEE J Quantum Electron 35:970
65. Fischer A, Andersen O, Yousefi M, Stolte S, Lenstra D (2000) Experimental and theoretical study of filtered optical feedback in a semiconductor laser. IEEE J Quantum Electron 36:375
66. Lang R, Kobayashi K (1980) External optical feedback effects on semiconductor injection laser properties. IEEE J Quantum Electron 16:347
67. Erzgräber H, Krauskopf B, Lenstra D, Fischer APA, Vemuri G (2006) Frequency versus relaxation oscillations in a semiconductor laser with coherent filtered optical feedback. Phys Rev E 73:055201(R)
68. Ahlborn A, Parlitz U (2004) Stabilizing unstable steady states using multiple delay feedback control. Phys Rev Lett 93:264101
69. Ahlborn A, Parlitz U (2005) Controlling dynamical systems using multiple delay feedback control. Phys Rev E 72:016206
70. Ahlborn A, Parlitz U (2006) Laser stabilization with multiple-delay feedback control. Opt Lett 31:465
71. Ahlborn A, Parlitz U (2007) Controlling spatiotemporal chaos using multiple delays. Phys Rev E 75:65202
72. Kyrychko YN, Blyuss KB, Hövel P, Schöll E (2009) Asymptotic properties of the spectrum of neutral delay differential equations. Dyn Sys 24:361
73. Blyuss KB, Kyrychko YN, Hövel P, Schöll E (2008) Control of unstable steady states in neutral time-delayed systems. Eur Phys J B 65:571
74. Johnston GA, Hunt ER (1993) Derivative control of the steady state in Chua's circuit driven in the chaotic region. IEEE Trans Circuits Syst 40:833
75. Parmananda P, Rhode MA, Johnson GA, Rollins RW, Dewald HD, Markworth AJ (1994) Stabilization of unstable steady states in an electrochemical system using derivative control. Phys Rev E 49:5007

76. Parmananda P, Eiswirth M (1996) Stabilizing unstable fixed points using derivative control. J Phys Chem 100:16568
77. Lu W, Yu D, Harrison RG (1996) Control of patterns in spatiotemporal chaos in optics. Phys Rev Lett 76:3316
78. Dahlem MA, Schneider FM, Schöll E (2008) Failure of feedback as a putative common mechanism of spreading depolarizations in migraine and stroke. Chaos 18:026110
79. Dahlem MA, Hiller G, Panchuk A, Schöll E (2009) Dynamics of delay-coupled excitable neural systems. Int J Bifur Chaos 19:745
80. Schneider FM Beeinflussung von neuronalen (2008) Erregungswellen durch raum-zeitliche Rückkopplung., Master's thesis, Technische Universität Berlin
81. Guzenko PY, Hövel P, Flunkert V, Fradkov AL, Schöll E (2008) Adaptive tuning of feedback gain in time-delayed feedback control. In: Fradkov A, Andrievsky B (eds) Proceedings of 6th EUROMECH nonlinear dynamics conference (ENOC-2008). IPACS Open Access Library http://lib.physcon.ru (e-Library of the International Physics and Control Society)
82. Yu X (1997) Tracking inherent periodic orbits in chaotic system via adaptive time delayed self-control. In: Proceedings of the 36th IEEE conference on decision and control vol 1, pp 401
83. Guzenko PY, Fradkov AL (1997) Gradient control of Henon map dynamics. Int J Bifur Chaos 7:701
84. Fradkov AL, Guzenko PY, Pavlov A (2000) Adaptive control of recurrent trajectories based on linearization of Poincare map. Int J Bifur Chaos 10:621
85. Astrov YA, Fradkov AL, Guzenko PY (2005) Suppression of a noise-induced transition by feedback control. In: Physics and control, 2005. Proceedings 2005 International Conference. IEEE, Piscataway, NJ, US, pp 662–667
86. Kakmeni FMM, Bowong S, Tchawoua C (2006) Nonlinear adaptive synchronization of a class of chaotic systems. Phys Lett A 355:47
87. Liao T-L, Lin S-H (1999) Adaptive control and synchronization of Lorenz systems. J Frankl Inst 336:925
88. Hale JK (1971) Functional differential equations. Applied mathematical sciences, vol 3. Springer, New York
89. Just W, Bernard T, Ostheimer M, Reibold E, Benner H (1997) Mechanism of time-delayed feedback control. Phys Rev Lett 78:203
90. N Baba: Stabilisierung instabiler räumlicher Muster durch zeitverzögerte Rückkopplung mit räumlichen Filtern. Master's thesis, Technische Universität Berlin (2001)
91. Amann A, Schöll E, Just W (2007) Some basic remarks on eigenmode expansions of time-delay dynamics. Physica A 373:191
92. Wünsche HJ, Schikora S, Henneberger F (2008) Noninvasive control of semiconductor lasers by delayed optical feedback. In:Schöll E, Schuster HG (eds) Handbook of chaos control. Wiley, VCH, Weinheim, second completely revised and enlarged edition
93. Erzgräber H, Krauskopf B, Lenstra D (2007) Bifurcation analysis of a semiconductor laser with filtered optical feedback. SIAM J Appl Dyn Syst. 6:1
94. Erzgräber H, Lenstra D, Krauskopf B, Fischer APA, Vemuri G (2007) Feedback phase sensitivity of a semiconductor laser subject to filtered optical feedback: experiment and theory. Phys Rev E 76: 026212
95. Erzgräber H, Krauskopf B (2007) Dynamics of a filtered-feedback laser: influence of the filter width. Opt Lett 32:2441
96. Green K Krauskopf B (2006) Mode structure of a semiconductor laser subject to filtered optical feedback. Opt. Commun. 258:243
97. Fischer APA, Yousefi M, Lenstra D, Carter MW, Vemuri G (2004) Filtered optical feedback induced frequency dynamics in semiconductor lasers. Phys Rev Lett 92:023901
98. Fischer APA, Yousefi M, Lenstra D, Carter MW, Vemuri G (2004) Experimental and theoretical study of semiconductor laser dynamics due to filtered optical feedback. IEEE J Sel Top Quantum Electron 10:944

99. Yousefi M, Lenstra D, Vemuri G (2003) Nonlinear dynamics of a semiconductor laser with filtered optical feedback and the influence of noise. Phys Rev E 67:046213
100. Illing L, Gauthier DJ (2006) Ultra-high-frequency chaos in a time-delay electronic device with band-limited feedback. Chaos 16: 033119
101. Wacker A (2002) Semiconductor superlattices: a model system for nonlinear transport. Phys Rep 357:1
102. Amann A (2003) Nonlinear and chaotic front dynamics in semiconductor superlattices. Ph.D. thesis, Technische Unversität Berlin
103. Wieczorek S, Krauskopf B, Lenstra D (1999) Unifying view of bifurcations in a semiconductor laser subject to optical injection. Opt Commun 172:279
104. Krauskopf B, Lenstra D (eds) (2000) Fundamental issues of nonlinear laser dynamics. In: AIP conference proceedings, vol 548. American Institute of Physics, Melville, New York
105. Wieczorek S, Krauskopf B, Lenstra D (2002) Multipulse excitability in a semiconductor laser with optical injection. Phys Rev Lett 88:063901
106. Wieczorek S, Krauskopf B, Simpson T, Lenstra D (2005) The dynamical complexity of optically injected semiconductor lasers. Phys Rep 416:1

http://www.springer.com/978-3-642-14109-6

Control of Complex Nonlinear Systems with Delay
Hövel, P.
2010, XVI, 253 p., Hardcover
ISBN: 978-3-642-14109-6